Lamellar Mesophase of Poly(ethylene oxide)–Poly(propylene oxide)–Poly(ethylene oxide) Melts and Water-Swollen Mixtures

Kell Mortensen*

Department of Solid State Physics, Risø National Laboratory, DK-4000 Roskilde, Denmark

Wyn Brown

Department of Physical Chemistry, Uppsala University, S-75121 Uppsala, Sweden

Erling Jørgensen

Chemistry Department, Roskilde University Center, Roskilde, Denmark

Received August 9, 1994; Revised Manuscript Received November 21, 1994[⊗]

ABSTRACT: Triblock copolymers of poly(ethylene oxide) (PEO) and poly(propylene oxide) (PPO) form lamellar mesophases at low temperatures. The order-to-disorder transition is closely related to the melting transition of the PEO subunit. When water is incorporated into the copolymer melt, a single phase is formed at high temperatures, which is possibly a lamellar mesophase, formed as a consequence of the hydrophobic PPO blocks. At low temperatures two phases are present, one of which is similar to the high temperature phase while the other is similar to the lamellar melt, but swollen up to 10%.

I. Introduction

The phase behavior of block copolymers has recently attracted great interest, as a result of both the commercial utility and the novel physical properties. Especially, many studies have been performed on amorphous diblock copolymers[1] in which the mesophase formation is determined by the Flory–Huggins interaction parameter, fluctuations, and conformational symmetry.

Mesophase formation can also be driven by other effects, as, for example, the tendency of one of the blocks to crystallize, which will be shown below. Studies of systems of crystalline blocks are rather rare and not well understood. Such polymers have, however, great technological importance. A number of commercial block copolymers are based on poly(ethylene oxide) which crystallizes at a low temperature depending on the molecular weight as well as the structure of the surrounding blocks. Such copolymers are, for example, utilized as polymer surfactants for viscosity control, etc. It is therefore important to know how the incorporation of a solvent affects the crystalline mesophase of the melt.

In the present study, we describe an experimental study of triblock copolymers of poly(ethylene oxide) and poly(propylene oxide), both in the melt and with water as a diluent. The mesophase of the melt appears to be lamellar. Upon increasing the water content, the mesophase melting (order-to-disorder) transition temperature decreases. Moreover, the lamellar mesophase is swollen to some limiting value, when the solvent is introduced.

II. Experimental Section

A. Material. The triblock copolymer, poly(ethylene oxide)–poly(propylene oxide)–poly(ethylene oxide),

$$HO[CH_2CH_2O]_{25}[CH(CH_3)CH_2O]_{40}[CH_2CH_2O]_{25}H$$

or PEO–PPO–PEO, abbreviated P85, was obtained from BASF Corp., Wyandotte, MI, and used without further purification. The material has a declared molecular weight of 4500, 2200 for the PEO component and 2300 for PPO. The solutions were prepared at ambient temperature and then heated to roughly 60 °C, to make homogeneous samples. Deuterium oxide, D_2O, was used in order to get good contrast and a low background in the neutron scattering experiments. The solutions discussed below are all given in weight percent (wt %).

B. Small-Angle Neutron Scattering. Small-angle neutron scattering experiments were performed using the Risø–SANS facility, which is a flexible instrument covering scattering vectors from 0.002 to 0.5 $Å^{-1}$, with variable neutron wavelength resolution.

The samples were mounted in sealed quartz containers (Suprasil from Hellma, FRG), with a 1 mm flight path.

The experiments were performed using neutron wavelengths (λ) of 3, 6, and 10 Å, with 1, 3, and 6 m sample-to-detector distances, respectively. The neutron wavelength resolution was $\Delta\lambda/\lambda = 0.18$, the neutron beam collimation was determined by the pinhole sizes of 16 and 7 mm diameter at the source and sample positions, respectively, and collimation lengths were equal to the sample-to-detector distance.

The scattering data were corrected for the background arising from the quartz cell and from other sources, as measured with the neutron beam blocked by plastic containing boron at the sample position. The incoherent scattering from H_2O was used to determine deviations from a uniform detector response and to convert the data into absolute units.

The scattering patterns discussed in the present paper are all azimuthally isotropic. The data have been reduced by azimuthally averaging to the one-dimensional $I(q)$ scattering functions which are only dependent on the absolute value of $\bar{q}$, where $\bar{q}$ is given by the scattering angle θ and the neutron wavelength λ: $|\bar{q}| = q = (4\pi/\lambda)\sin(\theta/2)$.

C. Light Scattering. Dynamic light scattering measurements were made on the P85 melt as well as on concentrated P85 solutions. The scattering cells (10-mL sealed cylindrical ampules) were immersed in a large-diameter thermostated bath of index-matching liquid (silicon oil). The polarized (V_V) DLS measurements, in the self-beating (homodyne) mode, were performed using a frequency-stabilized Coherent Innova Ar-ion laser operating at 488 nm with adjustable output power. The light was vertically polarized with a Glan–Thompson polarizer, with an extinction coefficient better than 10^{-6}. The detector optics employed a 4-μm-diameter monomodal fiber coupled to an ITT FW130 photomultiplier the output of which was digitized by an ALV-5000 digital multiple-τ autocorrelator, Langen GmbH, with 288 exponentially spaced channels. It has a minimum real time sampling time of 0.2 μs and a

---

[⊗] Abstract published in *Advance ACS Abstracts,* February 1, 1995.

0024-9297/95/2228-1458$09.00/0

maximum of about 100 s. The intensity autocorrelation function, $g^{(2)}(t)$, was measured at different angles. In the present study, in most cases, the temperature was 80 °C and was controlled to within ±0.02 °C.

Measurements of depolarized dynamic light scattering were also made where the scattered light passed through a Glan−Thompson polarizer with an extinction coefficient better than 10^{-7}, whose orientation was adjusted to give the minimum intensity for a dilute solution of a high molecular weight polystyrene in ethyl acetate. The DLS data were analyzed by nonlinear regression procedures. The various models used in the fitting procedures are expressed with respect to $g^{(1)}(t)$, while the fitting was performed with respect to the measured $g^{(2)}(t)$, described as

$$g^{(2)}(t) - 1 = \beta|g^{(1)}(t)|^2 \qquad (1)$$

where β is a nonideality factor which accounts for the deviation from ideal correlation. $g^{(1)}(t)$ can be written as the Laplace transform of the distribution of relaxation rates, $G(\Gamma)$:

$$g^{(1)}(t) = \int_0^{\infty} G(\Gamma)\exp(-\Gamma t)\,\mathrm{d}\Gamma \qquad (2)$$

where Γ is the relaxation rate and t is the lag time. For relaxation times, τ, eq 2 will be expressed as

$$g^{(1)}(t) = \int_{-\infty}^{\infty} \tau A(\tau)\exp(-t/\tau)\,\mathrm{d}(\ln\tau) \qquad (3)$$

where $\tau A(\tau) \equiv \Gamma G(\Gamma)$ in the logarithmic scale. $\tau A(\tau)$ was obtained by regularized inverse Laplace transformation of the dynamic light scattering data using a constrained regularization calculation algorithm called REPES, as incorporated in the analysis package GENDIST (see ref 9). This algorithm directly minimizes the sum of the squared differences between experimental and calculated $g^{(2)}(t)$ functions. It allows the selection of a "smoothing parameter", probability to reject (the higher the probability to reject, the greater the smoothing). A value of 0.5 was chosen in all analyses.

It is remarked that, in the present studies, there is an insignificant difference between the correlogram shapes and the positioning of the depolarized (V_H) and polarized (V_V) correlograms on the log-time axis.

The temperature of 80 °C was selected for the majority of the DLS measurements since preliminary studies showed that glass-clear mixtures with water existed at this temperature over the whole concentration range up to and including the melt.

The light source for the static light scattering was a 3-mW He−Ne laser (λ = 633 nm). The optical constant for vertically polarized light is

$$K = 4\pi n_0(\mathrm{d}n/\mathrm{d}c)^2/N_A\lambda^4$$

where n_0 is the solvent refractive index, dn/dc the refractive index increment which was measured using a specially constructed differential refractometer with Rayleigh interference optics ((dn/dc) = 0.131 mL/g at 633 nm), and N_A is Avogadro's number. R_θ is the Rayleigh ratio obtained by calibration measurements with benzene: $R_{90^\circ} = 11.85 \times 10^{-6}$ cm^{-1} at 25 °C.

D. Viscosity Measurements. Steady shear viscosities were measured at 60, 70, and 80 °C using a Bohlin VOR rheometer (Lund, Sweden). The Couette geometry (C14) was used at shear rates between 0.1 and 100 s^{-1}. The measured viscosities were independent of shear rate in the investigated range.

III. Results and Discussion

A. PEO−PPO−PEO Melt. *1. Neutron Scattering.* Figure 1 shows the scattering function of the P85 melt as observed at temperatures between T = 7 °C and T = 80 °C. The scattering function clearly reveals lamellar structure at low temperature, with both first- and second-order peaks. The lamellar periodicity is $d = 2\pi/q_0$ = 230 Å, where q_0 = 0.0272 Å^{-1} is the scattering momentum of the first-order peak. The additional small-angle scattering close to q = 0 reflects the fact that the P85 melt is incorporated with vacancies, which can be observed visually. The lamellar spacing is very large relative to the unimer radius of gyration R_g = 17 Å,[2] indicating highly stretched copolymers. Equivalent results were recently obtained in a related block copolymer in which the structure is "inverted" relative to P85, Pluronic-R 25R8, with PEO as the central block.[4]

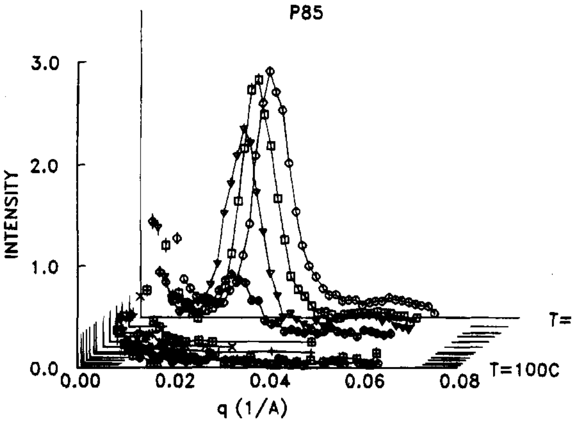

Figure 1. Neutron scattering function of the P85 melt as obtained at temperatures between T = 7 °C and T = 80 °C.

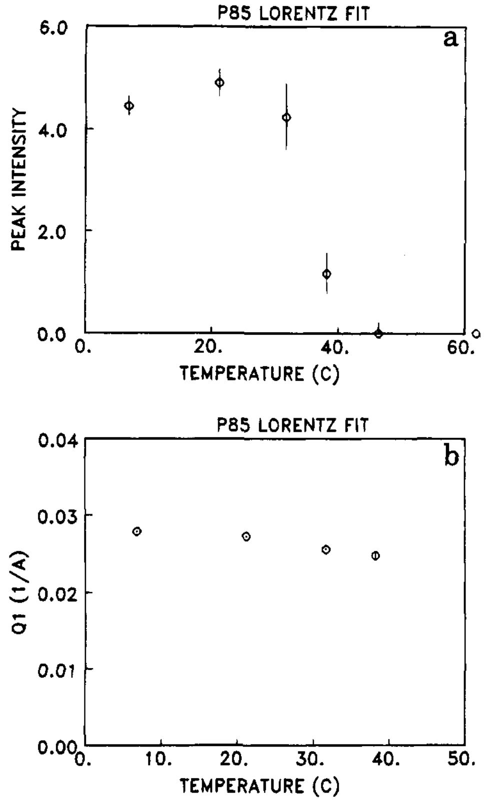

Figure 2. (a) Peak intensity I_0 and (b) corresponding wave vector q_0 as a function of temperature. The values are obtained by fitting a Lorentzian function to the experimental data.

The lamellar structure remains basically unaffected up to the melting temperature at T_m = 40 °C. Parts a and b of Figure 2 show respectively the peak intensity and momentum transfer as a function of temperature. The values are obtained by fitting a Lorentzian function to the experimental data.

Above T_m = 40 °C, no correlation peak is observable within the experimental resolution (Figure 1). This is quite different from observations on the amorphous block copolymers, where there is typically only a relatively small change in peak intensity on crossing the order–disorder transition (ODT). Above the ODT, a pronounced Leibler peak appears due to spatial concentration fluctuations.[5]

The peak intensity is, however, given not only by the amplitude of the concentration fluctuations but also by the scattering contrast between the two types of polymer blocks. In the P85 block copolymer melt, there is only significant contrast between PEO and PPO because the PEO block is crystalline whereas PPO is amorphous, thus resulting in a marked mass-density difference. At $T > T_m$ = 40 °C, PEO is also amorphous, and the scattering contrast vanishes. It is therefore not possible to detect eventual composition fluctuations above the PEO melting temperature with small-angle neutron scattering. Light scattering, as shown below, gives, however, an indication of important composition fluctuations in the disordered phase. Future studies should include partly deuterated copolymers, in which sufficient contrast for neutron scattering experiments can also be obtained in the amorphous regime.

2. *Light Scattering.* The P85 melt has a strongly anisotropic light scattering signal. Dynamic light scattering (DLS) measurements were made as a function of angle in both the V_V and V_H geometries. The V_V and V_H results were essentially identical, a result which is expected due to strong coupling.[3] The temperature range investigated covered in 10° steps the interval from 40 to 120 °C. Figure 3a shows the V_H intensity–intensity correlograms for the melt at 80 ° C and Figure 3b shows the corresponding Laplace inversion results. The correlograms are approximately q^2-dependent (Figure 3c), as was also observed to be the case with the "inverse" copolymer conformation, Pluronic-R 25R8.[4] Furthermore, the correlograms are single exponential (the exponent for fits to a stretched exponential is very close to unity), whereas most polymeric melts, which exhibit anisotropy due to segmental orientation relaxation, are typified by broad, q-independent, relaxation distributions.

The most ready interpretation is that the large anisotropy derives from the microstructure of domains which are rather homogeneous in overall size and which can move diffusively in the melt. A similar description was recently given by Fytas et al.[6] for an asymmetric diblock copolymer in solution close to the order-to-disorder transition (ODT) temperature.

The temperature dependence of the relaxation rate in the melt is small and should primarily depend on the viscosity of the medium. The latter (expressed in Pa s) is given for the melt over the limited range 60–80 °C by the relationship:

$$\ln(\eta) = -12.175 + 3707T^{-1} \tag{4}$$

where T is in Kelvin.

Together with the macroscopic viscosity, it is possible to estimate an apparent domain dimension using the Stokes–Einstein equation. With η = 0.188 Pa s (at 80 °C), $(R_h)_{app}$ = 220 nm. This is an estimate of the size of the "islands" moving in the melt and which are probably present in low number density. For this reason $(R_h)_{app}$ should be close to the true size which would exist in the absence of interparticle interactions.

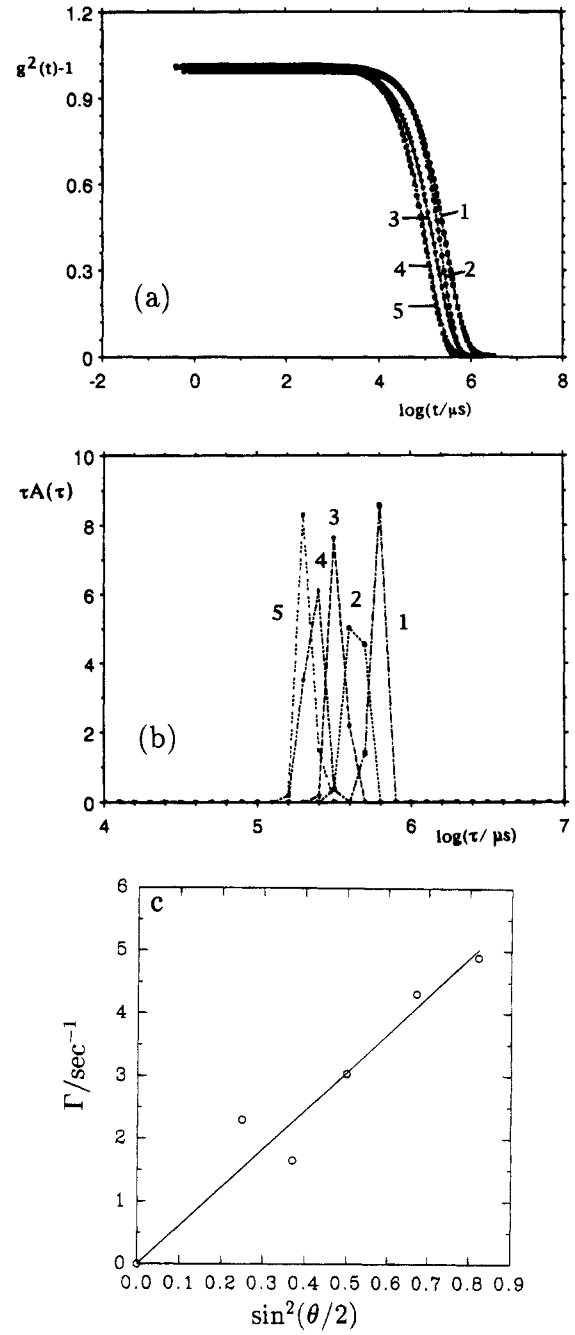

Figure 3. (a) Depolarized correlograms for the P85 melt at 80 °C at different angles. Peaks from right to left: (1) 60°; (2) 75°; (3) 90°; (4) 110°; (5) 130°. (b) Inverse Laplace transformation of the correlograms in Figure 3a. Peaks from right to left: (1) 60 °; (2) 75°; (3) 90°; (4) 110°; (5) 130°. (c) Plot of the relaxation rate (Γ/s^{-1}) versus sin^2 (Θ/2) obtained from the ILT analyses of the correlograms in Figure 3a.

B. PEO–PPO–PEO Melt Incorporated with Water. 1. *Neutron Scattering.* Incorporating small amounts of water (<20%) into the P85 melt, results in an homogeneous single-phase system above room temperature (depending on concentration) but in a two-phase system at low temperatures (Figure 4). In the low-temperature two-phase system, one phase is lamellar and quite similar to the pure melt, but swollen by 9 and 11% respectively for 10 and 20% water. The other phase of the low-temperature system is similar to the single phase observed at higher temperatures (or higher water concentrations).

Figures 5–7 show the detailed temperature dependencies of the scattering functions of 90%, 80%, and 50%

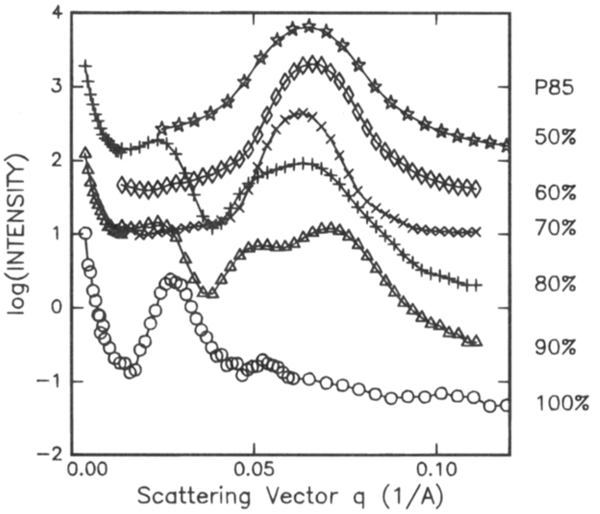

Figure 4. Neutron scattering functions as observed at $T = 7$ °C for P85, and P85 diluted to polymer concentrations of 90%, 80%, 70%, 60%, and 50% with water (D_2O).

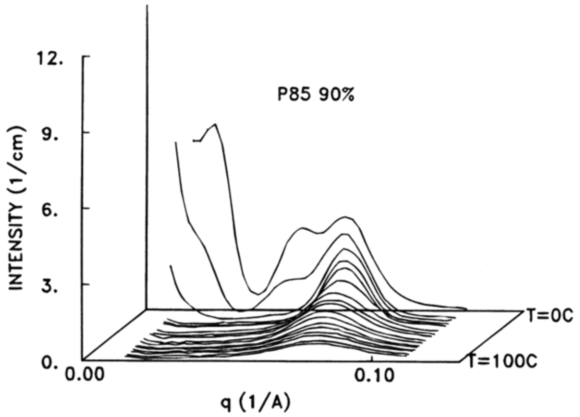

Figure 5. Neutron scattering functions of a 90% concentrated P85 mixture as obtained at temperatures between $T = 7$ °C and $T = 90$ °C.

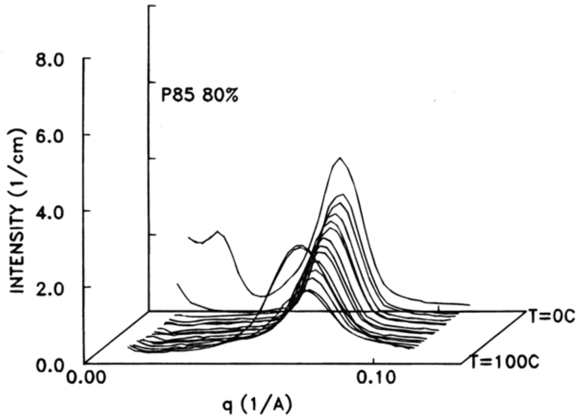

Figure 6. Neutron scattering functions of a 80% concentrated P85 mixture as obtained at temperatures between $T = 7$ °C and $T = 90$ °C.

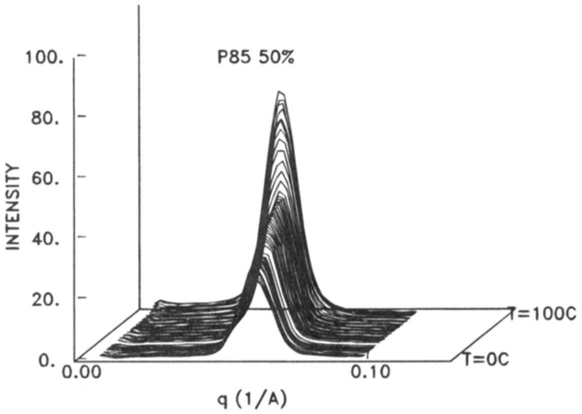

Figure 7. Neutron scattering functions of a 50% concentrated P85 mixture as obtained at temperatures between $T = 5$ °C and $T = 90$ °C.

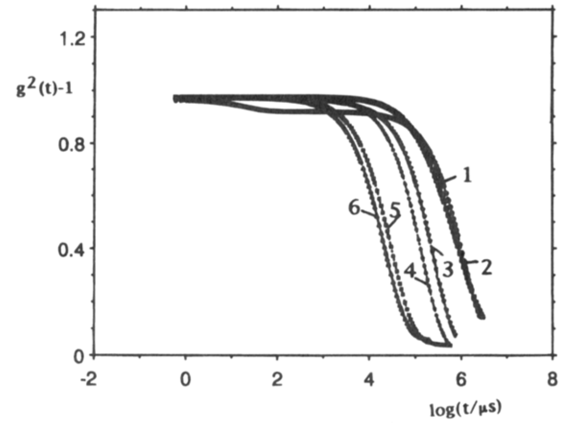

Figure 8. Correlogram (V_H) for $c = 90\%$ P85 at angle 90°. From right to left the temperatures are as follows: (1) 60, (2) 70, (3) 75, (4) 78, (5) 80, (6) 90 °C.

polymer concentrations, respectively. For temperatures above 20 and 15 °C for respectively the 90% and 80% samples, a single correlation peak is the dominant feature of the scattering function. For water concentrations of 50% and more, this single phase is observed over the temperature range studied, i.e., up to ~90 °C. The phase may also be lamellar. Clearly, the scattering pattern becomes anisotropic when the sample is exposed to shear and results in a characteristic pattern with two symmetrical broad arcs. We conclude that it is lamellar because we have not been able to observe any hexagonal pattern in orientations perpendicular to the shear plane, which should appear in the case of a hexagonally packed rod structure. This lamellar phase is, however, quite different from the lamellar melt.

In the lamellar melt, the structure is markedly dominated by the crystalline PEO blocks. This crystallinity results in highly stretched PEO chains, giving a relatively large lamellar periodicity. Moreover, we argue that PEO crystallinity is the driving force for the lamellae formation, as the PEO blocks "aggregate" in the crystalline subunits.

The lamellar phase of the diluted samples is quite different. Here the driving force is the interaction between the hydrophobic PPO and water, resulting in aggregation of the PPO blocks into a lamellar form. The periodicity of this "inverted lamellar structure" is of the order of 90 Å and depends only weakly on concentration and temperature.

At temperatures close to 78 °C for 50% and 90 °C for 80% water, a marked change in the scattering pattern appears. The scattering function is still dominated by a single pronounced correlation peak but is significantly more intense. It is not clear from the present study what this high-temperature phase consists of.

2. Light Scattering. Figure 8 shows correlation functions ($g^{(2)}(t) - 1$) for $c = 90\%$ polymer concentration, as measured between 60 and 90 °C at an angle of 90°. Except for the lowest temperature measured, the data show a single-exponential decay. At 60 °C, a signature of an additional fast mode appears. Upon further

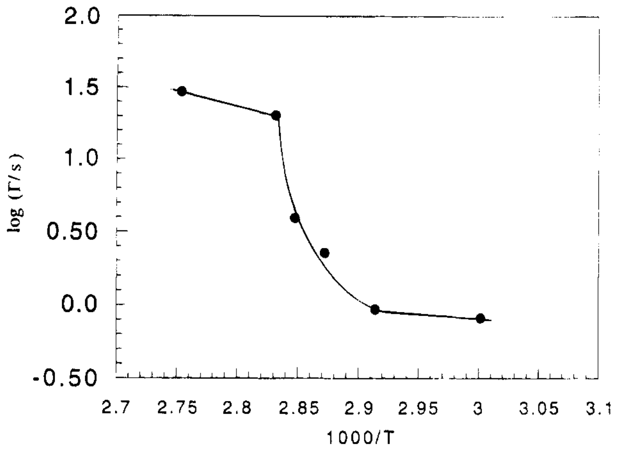

Figure 9. Temperature dependence (Kelvin) of the slow relaxation time for c = 90% P85.

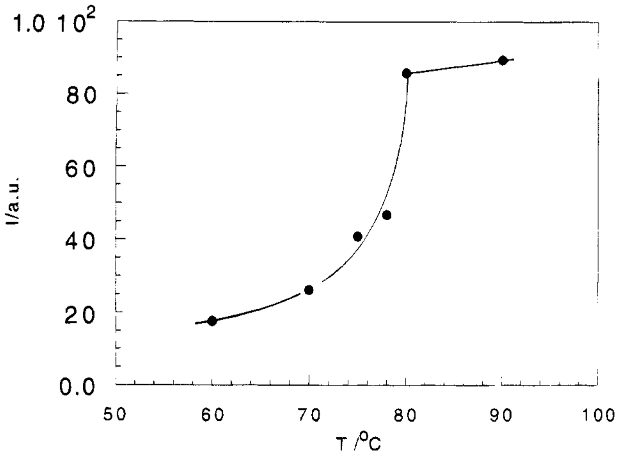

Figure 10. Intensity (arbitrary units) versus temperature (°C) for c = 90% P85.

dilution, however, the fast mode becomes more pronounced and remains at higher temperatures. The slow mode probably derives from the formation of domains in the incipient ordered phase, which is probably lamellar as discussed above. The relaxation time of the slow mode at 80 °C decreases with increasing concentration, indicating that the domain size increases as the water content is increased.

Figure 9 depicts relaxation rates for the slow mode in the c = 90% solution. These data were obtained from the position of the peaks subsequent to ILT of the data in Figure 8. The scattering vector dependence of the relaxation rate has a q^2 dependence, indicating diffusive character. The data of Figure 9, together with those in Figure 10 for the total scattered intensity, show that there is a transition located at approximately 79 °C. It is likely that this corresponds to the same transition as that observed for lower polymer concentrations in the neutron scattering data. Transitions of this character were, however, not observed using light scattering for the 80 and 70% samples in the temperature range studied (40–90 °C). The nature of the transition is at present unclear.

The fast-decaying mode has a higher relative amplitude upon dilution with water. Data are shown in Figures 11 and 12 for respectively c = 80% and c = 70% solutions of P85 at different scattering vectors and measured in the V_H geometry.

Comparison of the correlograms for the concentrated solutions in Figures 11 and 13a with those for the melt shown in Figure 3a shows that the addition of diluent

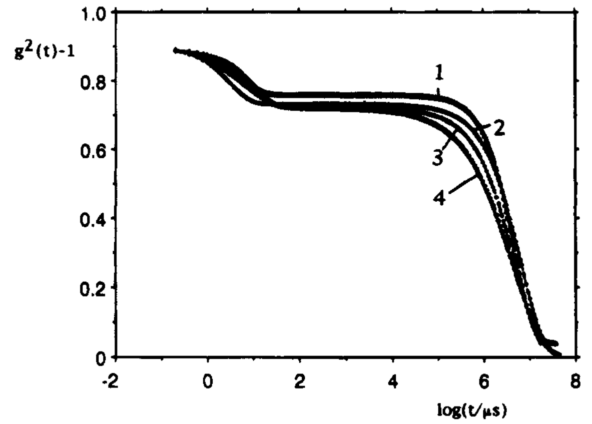

Figure 11. Depolarized correlograms (V_H) at c = 80 wt % P85 at 80 °C. From right to left, angles are as follows: (1) 80, (2) 90, (3) 105, (4) 120 °C.

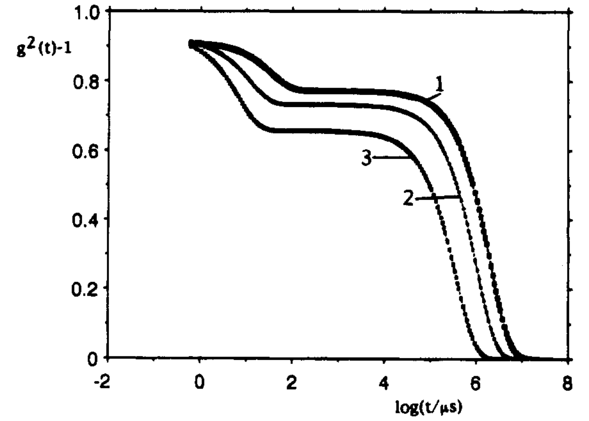

Figure 12. Depolarized (V_H) correlograms for c = 70 wt % at 80 °C at angles from right to left: (1) 70, (2) 120, (3) 135°. Both relaxation modes are q^2-dependent (diffusive).

to produce concentrations lower than or equal to c = 80% leads to a substantial decrease in the relaxation rate of the slow mode. It was concluded above that the diffusive mobility in the melt in the depolarized geometry corresponds to the diffusion of anisotropic domains of magnitude 200 nm by analogy with findings in similar systems.[4,6] Since the addition of water would be expected to decrease frictional interactions characterizing the diffusion of domains, it follows that the domain size must increase significantly in the presence of diluent above the level of 20%. The relative amplitude of the fast mode increases with increasing scattering vector (q) and the corresponding relaxation rate is q^2-dependent, i.e., diffusive, as is the slow mode.

Figure 13a shows the correlation functions for concentrated P85 samples (70, 80, and 90% copolymer) in water (D_2O), as obtained at 80 °C.

For c = 90%, the correlation function is close to a single exponential, as observed in the P85 melt. For c = 70% and c = 80%, however, the correlograms become bimodal. This trend is further emphasized on decreasing the copolymer concentration, as seen in Figure 13b.

The decay time of the slower relaxation is approximately independent of concentration for c up to roughly 50%. This suggests that the domain size in the low concentration samples does not vary significantly and that only their number density changes with concentration. Since strong birefringence is observed for these intermediate concentrations, it is concluded that the slow mode derives from the formation of domains in the

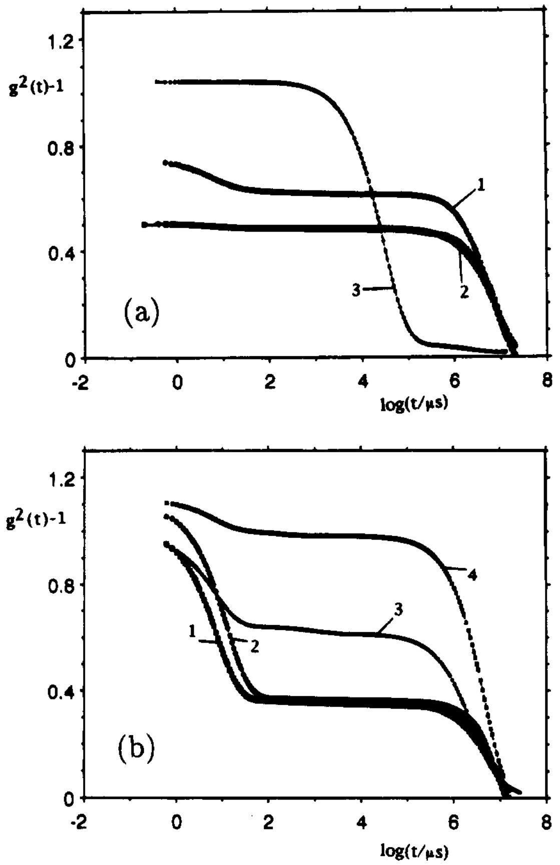

Figure 13. (a) Dynamic light scattering polarized (V_V) correlograms for P85 at 80 °C from right to left at concentrations (1) 70, (2) 80, and (3) 90%. (b) Data analogous to that of Figure 13a. Correlograms (V_V) from right to left at concentrations (1) 35, (2) 45, (3) 50, and (4) 60%.

incipient hexagonal phase, which has previously been identified by SANS measurements.[7]

The fast mode is diffusive. Upon even further dilution, the correlation function eventually becomes single exponential. This diffusive relaxation is interpreted as reflecting the screening length characterizing the hydrodynamic interactions in the close-packed micellar phase.[8]

IV. Conclusion

In conclusion we have shown that the triblock copolymer of PEO–PPO–PEO (P85) at low temperatures forms a lamellar mesophase, which is a result of self-assembling PEO blocks. The PEO aggregation is driven by the tendency to form crystalline PEO domains. The copolymers are highly stretched in the lamellar phase. The lamellar periodicity is 230 Å as compared to the polymer radius of gyration of 17 Å. Significant microstructure is present in the disordered phase, as is experimentally evident from the anisotropic light scattering data.

Upon dilution, water presumably condenses into the PEO-rich domains, forming a second type of lamellar phase, where the driving force is the self-assembly of hydrophobic PPO blocks. The periodicity of these lamellae is of the order of 90 Å. At temperatures between roughly 10–40 (depending on polymer concentration) and 90 °C, the samples form a single glass-clear phase of these lamellae.

At low temperatures, a two-phase system represents the stable state, formed by domains of both types of lamellar structure. The melt lamellae are, however, somewhat swollen by the water. The transition temperature of this swollen melt-type of lamellar structure is lowered upon dilution with water and is not observed for polymer concentrations below approximately 70%. These phase behaviors are summarized in the phase diagram in Figure 14.

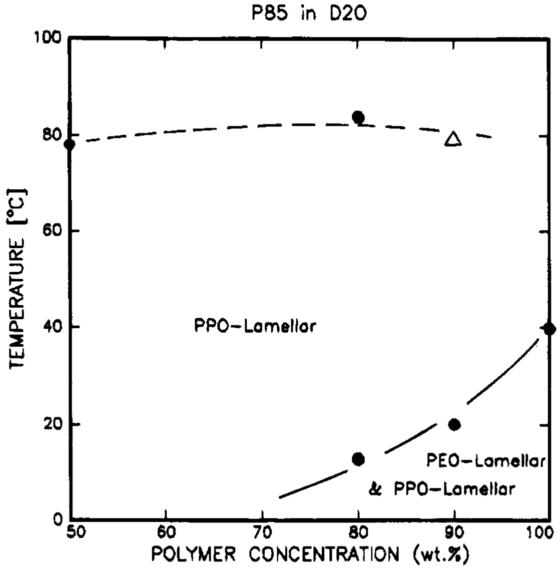

Figure 14. Phase behavior of P85–D_2O in the 50–100% polymer concentration. The PEO lamellar phase is formed as a consequence of PEO crystallization. The PPO lamellar phase is formed as a consequence of self-assembling PPO due to hydrophobic interactions. Closed symbols represent neutron results; open symbol represent light scattering.

Acknowledgment. The work has been supported by grants from the Danish and the Swedish Natural Science Research Councils. The P85 copolymers were provided by BASF-Denmark and BASF-Wyandotte, NJ.

References and Notes

(1) For a recent review, see: Bates, F. S.; Schultz, M. F.; Khandpur, A. K.; Förster, S.; Rosedale, J. H.; Almdal, K.; Mortensen, K. *Trans. Faraday Soc.* in press.

(2) Mortensen, K.; Pedersen, J. S. *Macromolecules* **1993**, *26*, 805.

(3) Wang, C. H.; Fischer, E. W. *J. Chem. Phys.* **1985**, *82*, 632.

(4) Mortensen, K.; Brown, W.; Jørgensen, E. *Macromolecules* **1994**, *27*, 5654.

(5) Leibler, L. *Macromolecules* **1980**, *1980*, *13*, 1602.

(6) Jian, T.; Anastasiadis, H.; Fytas, G.; Adachi, K.; Kotaka, T. *Macromolecules* **1993**, *26*, 4706.

(7) Mortensen, K. *Europhys. Lett.* **1992**, *19*, 599.

(8) Brown, W.; et al. To be published.

(9) Schillén, K.; Brown, W.; Johnsen, R. M. *Macromolecules* **1994**, *27*, 4825.

MA941191R